JOURNAL OF CATALYSIS 127, 51–66 (1991)

Relation between Properties and Performance of Zeolites in Paraffin Cracking

A. F. H. WIELERS, M. VAARKAMP, AND M. F. M. POST

Koninklijke/Shell-Laboratorium Amsterdam (Shell Research B.V.), Badhuisweg 3, 1031 CM Amsterdam, The Netherlands

Received February 19, 1990; revised August 10, 1990

The effects of zeolite structure, acid site density, and reaction temperature on the mode of *n*-hexane cracking have been studied. The results can be consistently explained in terms of the occurrence of two different cracking routes, viz. the classical β-scission route and the monomolecular protolytic pathway. The relative contribution of each of the two cracking routes is expressed by the "cracking mechanism ratio" (CMR): a high value of this index points to a relatively high contribution of the protolytic cracking route, whereas a low value indicates that the classical β-scission route is the main cracking pathway. With increasing temperature, decreasing aluminium content, and decreasing pore dimensions the relative contribution of the (monomolecular) protolytic cracking route increases as compared to the (bimolecular) classical route. On the basis of these results the variation of the constraint index (i.e., the ratio of the first-order rate constants for conversion of *n*-hexane and 3-methylpentane) with aluminium content and reaction temperature can be easily rationalized. Furthermore, the present results also provide an explanation for the change in the activation energy of *n*-hexane cracking with aluminium content in zeolite ZSM-5 (MFI). Finally, it is tentatively concluded that the classical cracking route is favoured by the presence of two adjacent acid sites and by low reaction temperatures. Consequently, the relation between the reaction rate constant and the lattice aluminium content changes with the reaction temperature; whereas at 811 K the cracking constant varies linearly with the aluminium content, at 623 K the order in the aluminium content increases to about 2. © 1991 Academic Press, Inc.

INTRODUCTION

In catalytic cracking solid acid materials are used as catalysts to convert vacuum distillates and residues into high-octane gasolines, diesel oil, and olefinic gases. Furthermore, catalytic cracking of paraffins is frequently used as a test reaction to assess the acidic properties of the acid catalyst. With regard to the nature of the acid-catalysed cracking reaction it is generally accepted that cracking proceeds via a bimolecular carbenium-ion chain mechanism involving a hydride-transfer step, followed by β-scission (*1–3*). However, recently various authors have found evidence that cracking may also proceed via another route, which has been called in the literature the monomolecular protolytic cracking route (*4–6*). Whereas the characteristic products of the classical β-scission route are propene and isobutane, the typical products of the protolytic cracking route are methane, ethene, ethane, and hydrogen.

Haag and Dessau (*4*) and Corma *et al.* (*5*) have suggested that protolytic cracking with zeolites proceeds via pentacoordinated carbonium ions formed upon protonation of a paraffin, analogously to reactions occurring in liquid superacids (*7, 8*). However, as the typical products of the protolytic cracking route are methane, ethene, and hydrogen, Corma (*9, 10*) suggested that this reaction proceeds via a radical cracking mechanism catalysed by nonframework aluminium ions present in the zeolite. Regardless of the exact mechanism of the protolytic cracking route, it is important to identify the properties of the zeolite and the reaction conditions affecting the relative contribution of this al-

0021-9517/91 $3.00
Copyright © 1991 by Academic Press, Inc.
All rights of reproduction in any form reserved.

ternative cracking pathway. Haag and Dessau (*4*) found that the protolytic cracking route is more favoured with the medium-pore zeolite ZSM-5 (MFI) than with the large-pore zeolite FAU(Y) and amorphous silica–alumina material. Furthermore, they showed that protolytic cracking becomes more prominent with increasing temperatures and decreasing reactant concentrations. Gianetto *et al.* (*11*) concluded that protolytic cracking is more pronounced with a silicon-rich FAU(Y) (Si/Al = 35 mol/mol) than with an aluminium-rich sample (Si/Al = 3 mol/mol). Mirodatos and Barthomeuf (*12*) suggested that protolytic cracking is favoured with small-pore zeolites and/or zeolites with a high tortuosity.

From the survey of the literature it thus appears that several factors determine the relative contributions of the two acid-catalysed cracking routes. In this work we have investigated in more detail the role of acid site density, the influence of zeolite structure and the effect of reaction temperature on the relative contributions of the two cracking routes. In order to facilitate the interpretation of the results we used well-defined zeolite catalysts. The effect of zeolite structure has been investigated with a series of four structurally different zeolites containing similar amounts of aluminium. The role of acid site density has been studied with a series of MFI samples differing in lattice aluminium content. *n*-Hexane (*n*-H) and 3-methylpentane (3-MP) cracking were used as test reactions.

EXPERIMENTAL

The cracking experiments were performed in a small microflow reactor. *n*-Hexane cracking experiments, performed to elucidate the effects of zeolite structure and acid site density on product selectivity, were carried out at 723 K and a pressure of 0.5 MPa using diluted *n*-hexane as feed (He/*n*-H = 4/1 mol/mol). Since the selectivity is a function of the conversion level, a meaningful comparison of selectivities can only be made at similar conversion levels, which condition was achieved by carefully adjusting the space velocity. Occasionally, *n*-H cracking was studied at lower pressures (total pressure 0.1 MPa; He/*n*-H = 4/1 mol/mol). Measurements of the constraint index (CI) were normally carried out at standard conditions as outlined in the Mobil publications (total pressure 0.1 MPa; He/(*n*-H + 3-MP) = 4/1 mol/mol) (*13, 14*). The CI is the ratio of the first-order rate constants for conversion of *n*-hexane and 3-methylpentane. When isomerisation within the feed was suspected, the experiments were performed using pure hexane isomers as feedstocks (vide infra).

Two series of ZSM-5 zeolites (MFI) with Si/Al molar ratios between 8 and 400 were prepared according to Mobil patents using either tetrapropylammonium bromide (TPABr) or hydroxide (TPAOH) as templating agent (*15*). The crystallinity of the MFI samples tested was 100%, except for the sample with Si/Al = 8 mol/mol, which contained traces of analcime. Zeolite ferrierite (FER) (Si/Al = 8 mol/mol) was synthesized according to an in-house developed procedure. Zeolite mordenite (MOR) (Si/Al = 8.5 mol/mol) was obtained from Union Carbide and ultrastable faujasite (Y, FAU) (Si/Al = 10 mol/mol) from Grace Davison. Relevant characteristics of the various zeolites are given in Table 1. The calcined (773 K for 16 h in air) zeolite samples were exchanged with a large excess of NH_4NO_3 at 363 K for 16 h, washed and dried at 393 K. Prior to the cracking experiments the catalysts were treated in the reactor with a stream of dried helium at 773 K for 2 h.

^{27}Al solid-state NMR showed that in the silicon-rich MFI samples (Si/Al > 10 mol/mol) all aluminium ions are present in tetrahedral positions. Owing to the presence of some amorphous material in aluminium-rich MFI sample (Si/Al = 8 mol/mol) this particular sample contains a small amount of non-framework aluminium. Whereas in the fresh

TABLE 1

Relevant Characteristics of the Zeolites used in the Various Experiments

Zeolite	Si/Al (mol/mol)	Crystallite size diameter (μm)	Source/ preparation route
FAU (Y)	10.5	≈1	Grace Davison
MOR	8.5	0.5–1	Union Carbide
FER	8	0.5–1	Homemade
MFI	8	0.5–1.5	Via TPABr route (*15*)
MFI	21	0.5–1.5	Do.
MFI	40	—	Do.
MFI	75	—	Do.
MFI	200	1–2	Do.
MFI	400	1–2	Do.
MFI	20	<0.1	Via TPAOH route (*15*)
MFI	25	2	Do.
MFI	30	<0.1	Do.
MFI	38	<0.2	Do.
MFI	45	—	Do.
MFI	65	0.13	Do.
MFI	100	1	Do.
MFI	130	0.2	Do.

MOR and FER samples all aluminium ions are located in tetrahedral frame-work positions, there is also a small amount of non-tetrahedrally coordinated aluminium present in FAU(Y).

RESULTS

Activity in n-Hexane Cracking

It is known (*16*) that at high temperatures (811 K, 538°C) the cracking rate is first order in *n*-hexane. From the results shown in Fig. 1 it can be concluded that also at lower reaction temperatures (673–573 K, 400–300°C) the cracking rate is first order in *n*-hexane. Thus, the apparent rate constant (k) can be calculated via the well-known formula $k = -\text{WHSV} \times \ln(1 - x)$, in which x is the conversion level.

Table 2 shows the conversion levels of four structurally different zeolites containing similar concentrations of aluminium (with all four zeolites the Si/Al molar ratio is between 8 and 10). The very high stability of zeolite MFI for *n*-H cracking allowed us to study excursions of temperature and/or space velocity in a single run, and check-backs at initial operating conditions were frequently carried out to verify that the zeolite had not suffered from aging during the

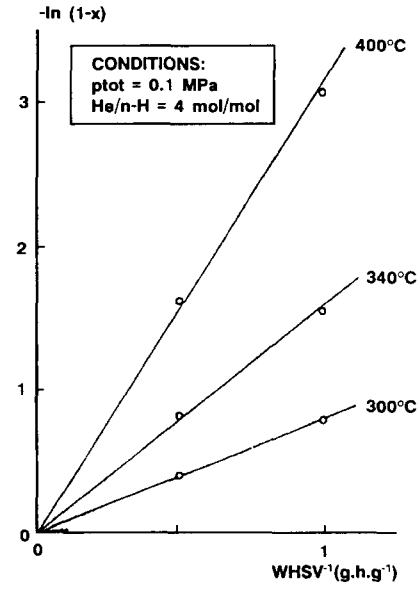

FIG. 1. Effect of space velocity on cracking rate of *n*-hexane over zeolite MFI (Si/Al = 38 mol/mol).

TABLE 2

Product Breakdown in Cracking of *n*-Hexane over Structurally Different Zeolites

Zeolite:	FER	MFI	MOR	FAU(VUS-Y)
Si/Al (mol/mol)	8	8	8.5	10.5
Conv. (%w)	9.4	14	7.3	10.3
WHSV (g/(g · h))	59	550	34	16
k_0 (g/(g · h))	5.9	83	2.6	1.7
k_{Al}	54	747	24	19
$\log(k_{Al})$	1.7	2.9	1.4	1.3
Selectivity (%mol)				
H_2	38.3	2.3	13.9	4.8
C_1	4.5	0.7	0	2.3
ΣC_2	22.8	6.7	5.9	5.3
C_2^0/C_2^{2-}	3.9	0.8	0.8	1.0
ΣC_3	26.7	59.0	59.9	38.6
C_3^0/C_3^{2-}	2.3	2.5	3.3	14.2
ΣC_4tot	6.8	25.3	9.7	13.6
ΣC_4^{2-}	4.8	14.8	4.9	6.8
Σn-C_4^{2-}	4.8	9.9	2.0	2.3
i-C_4^{2-}	0	4.9	2.9	4.5
ΣC_4^0	2.0	10.5	4.9	6.8
n-C_4^0	2.0	7.0	2.3	1.9
i-C_4^0	0	3.5	2.6	4.9
C_4^0/C_4^{2-}	0.4	0.7	1.0	1.0
i-C_4^0/n-C_4^0	0	0.5	1.1	2.5
CMR = $(C_1 + \Sigma C_2)/i$-C_4^0	∞	2.1	2.3	1.6
ΣC_5	0	3.4	1.8	6.6
ΣC_6 isomers	1	1.8	8.8	28.7

Note. Conditions: T = 723 K; He/*n*-H = 4 (mol/mol); P_{tot} = 0.5 MPa.

run. The other zeolite structures investigated (viz. FER, MOR, FAU), however, deactivated severely during operation, and therefore, on account of the different rates of deactivation, the activity was assessed by comparing the initial rate constants (k_0), which were found by extrapolation of the conversion vs time-on-stream curves to $t = 0$.

In Fig. 2 the normalized rate constants (k_{Al}) of the four structurally different zeolites are plotted as a function of the pore dimensions of the respective zeolite. Normalized rate constants were calculated at conversion levels of about 10% (Table 2) after correction for small differences in aluminium content according to $k_{Al} = k_0/\{Al/(Al + Si)\}$ and are assumed to be proportional to the intrinsic activity (turnover frequency) of the strong Brønsted acid sites of each particular zeolite sample. A volcano-type relation is observed between the catalytic activity and the dimensions of the pores: the medium-pore zeolite MFI exhibits a markedly higher activity than the large-pore zeolites MOR and FAU(Y) as well as the medium-pore zeolite FER. The volcano-type relation has also been found for *n*-pentane (*17*) and *n*-butane (*18*) cracking. However, Lombardo *et al.* (*19*) reported a different order for *n*-H cracking, viz. MOR ≫ FAU(Y) > MFI. The differences in activity have been ascribed to differences in intrinsic acidity (*19*), to variations in the concentration of the reactants in the pores (*20*), and to nest effects (*21*). In a forthcoming paper

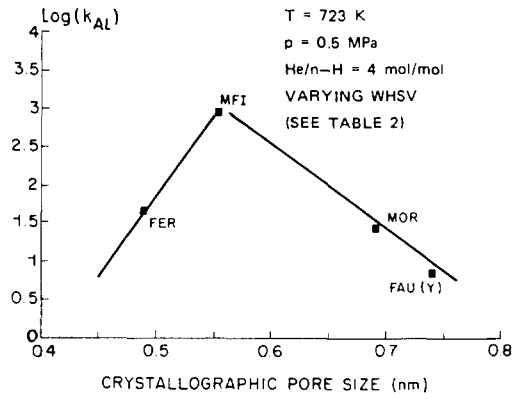

FIG. 2. Cracking activity of various structurally different zeolites.

we will present additional data and offer an explanation for the observed activity order (*22*).

Previously, it was shown that at 703 K with MFI samples containing crystallites with dimensions between 0.1 and 5 μm the *n*-H cracking rate is independent of the crystallite size (*23*). Therefore, we conclude that the rate constants found in the present work for *n*-H cracking over zeolite MFI reflect the true rate of the cracking reaction. Since diffusion limitations are not important for the medium-pore zeolite MFI in *n*-H cracking and since the crystallite sizes in the various zeolites are not too different, it can be concluded that the same should be true for the wide-pore zeolites MOR and FAU (Y) as well as for the medium-pore zeolite FER (the pore dimensions of zeolite FER are only slightly smaller than those of zeolite MFI).

Using the series of MFI zeolites with different aluminium contents the first-order rate constant for *n*-H cracking has been determined as a function of the aluminium content. Figure 3 and Table 3 show the results obtained at 723 K. It can be seen that the slope of the straight line obtained upon plotting log k_0 vs log(Al/(Al + Si)) is about 1.2, indicating that the apparent order in the aluminium content is about 1.2 at this temperature. The relation between the cracking rate constant and the aluminium content in zeolite MFI has been further investigated over a broad range of temperatures. The apparent order in aluminium content as calculated from these results is plotted as a function of temperature in Fig. 4. Also included are results reported in the literature. Surprisingly, the order increases from 1 to 2 when the temperature decreases from 811 to 623 K.

The effect of reaction temperature and aluminium content of MFI on *n*-H cracking activity can be inferred from the results given in Fig. 5, showing the activation energy as a function of Al content. Activation energies were obtained from Arrhenius plots. The temperature ranges studied typically spanned about 100 K and over this range the relation between ln k and $1/T$ could satisfactorily be approximated by a straight line. The average temperature at which the activation energy was determined increases with decreasing aluminium con-

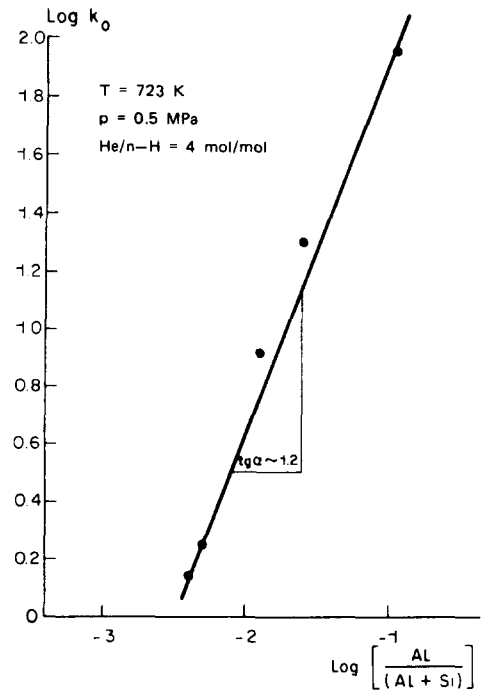

FIG. 3. Activity as a function of aluminium content for a series of H-MFI catalysts.

TABLE 3

Product Breakdown in Cracking of *n*-Hexane over Various MFI (ZSM-5) Zeolites containing Different Amounts of Aluminum

Zeolite:	Various MFI (ZSM-5)				
Si/Al (mol/mol)	8	40	75	200	400
Conv. (%w)	14	13.4	13.4	16.1	30.9
WHSV (g/(g · h))	550	131	65	20	4
k_0 (g/(g · h))	83	18.8	9.3	3.5	1.4
k_{Al}	747	772	711	706	592
$\log(k_{Al})$	2.9	2.9	2.9	2.8	2.8
Selectivity (%mol)					
H_2	2.3	1.0	6.9	9.1	9.9
C_1	0.7	0.5	2.5	3.8	3.1
ΣC_2	6.7	13.7	12.8	16.5	14.5
C_2^0/C_2^{2-}	0.8	0.8	1.0	1.8	1.5
ΣC_3	59.0	52.8	47.7	47.1	45.2
C_3^0/C_3^{2-}	2.5	2.6	2.4	2.0	2.4
ΣC_4tot	25.3	25.7	23.9	17.9	20.6
ΣC_4^{2-}	14.8	15.0	14.9	11.2	12.9
$\Sigma n\text{-}C_4^{2-}$	9.9	10.0	9.9	7.0	8.1
$i\text{-}C_4^{2-}$	4.9	5.0	5.0	4.2	4.8
ΣC_4^0	10.5	10.7	9.0	6.7	7.7
$n\text{-}C_4^0$	7.0	7.1	6.0	4.2	4.8
$i\text{-}C_4^0$	3.5	3.6	3.0	2.5	2.9
C_4^0/C_4^{2-}	0.7	0.7	0.6	0.6	0.6
$i\text{-}C_4^0/n\text{-}C_4^0$	0.5	0.5	0.5	0.6	0.6
$CMR = (C_1 + \Sigma C_2)/i\text{-}C_4^0$	2.1	3.9	5.1	8.1	6.1
ΣC_5	0	3.4	4.0	3.7	4.2
ΣC_6 isomers	1.0	2.8	3.1	1.9	2.6

Note. Conditions: T = 723 K; He/*n*-H = 4 (mol/mol); P_{tot} = 0.5 MPa.

tent in the MFI samples and is indicated in Fig. 5. The activation energy for *n*-hexane cracking decreases with increasing aluminium content and/or with decreasing temperature.

Selectivity for n-Hexane Cracking

The effect of zeolite structure on product selectivity can be inferred from the results shown in Table 2. Compared to the other zeolites, FER exhibits a relatively low selectivity for the formation of C_4 hydrocarbons and a high selectivity for the formation of hydrogen, methane, and C_2 hydrocarbons. In agreement with the formation of hydrogen, zeolite FER also exhibits a high selectivity for the formation of olefins. It is also interesting to note that with increasing pore dimensions the selectivity for C_6 isomers increases. Furthermore, with increasing pore dimensions, the olefinic content of the product molecules decreases.

The selectivity patterns (Table 3) of the various MFI catalysts differing in aluminium content indicate that the selectivity for the formation of hydrogen, methane, and C_2 hydrocarbons increases with decreasing aluminium content in the lattice. Moreover, the selectivity for the formation of olefins increases with decreasing aluminium content.

The effect of reaction temperature in the range 643 to 803 K on the selectivity in *n*-H cracking has been studied in more detail

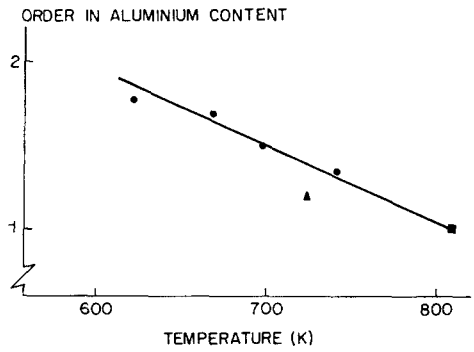

FIG. 4. Order in aluminium content of H-MFI catalysts as a function of temperature. (○) Measured under conditions as given in Ref. (*23*): P_{tot} = 0.1 MPa; p (*n*-H) = 0.02 MPa. (△) Measured under conditions used in this work: P_{tot} = 0.5 MPa; p (*n*-H) = 0.1 MPa. (■) Measured under conditions of α-test (Ref. (*16*)): P_{tot} = 0.1 MPa; p (*n*-H) = 0.013 MPa.

with H-MFI, having a Si/Al molar ratio of 45. It is evident from Fig. 6 that with increasing temperature the selectivity for the formation of C_3–C_5 decreases, whereas the selectivity for C_1 and C_2 increases. In this series of experiments the conversion decreases from about 80% (at the highest temperature) to about 30% (at the lowest temperature). The present results are in full agreement with data previously reported by Haag and Dessau (*4*).

Constraint Index

Figure 7 shows the variation of the constraint index of zeolite MFI as a function of the aluminium content and the reaction temperature. The majority of the results given in Fig. 7 were obtained using a two-component feed consisting of *n*-H and 3-MP as indicated in Refs. (*13, 14*). However, at lower temperatures and with aluminium-rich MFI samples isomerisation of hexanes is significant and, as a result, the interconversion of hexane isomers in the two-component feed may severely falsify the "true" constraint index at these conditions. Therefore at lower temperatures and with aluminium-rich samples, these problems were circumvented by using single-component feeds in order to unambiguously assess the "true" ratio of the rates of cracking. The constraint indices given in Fig. 7 accordingly reflect the actual ratio of cracking rates of the two hexane isomers and might therefore slightly deviate from the values that would be obtained using the conditions stated in the pertinent literature (*13, 14*). The results shown in Fig. 7 indicate that the CI decreases with increasing temperature and decreasing aluminium content.

DISCUSSION

Cracking Mechanisms

Cracking of paraffins at elevated temperatures may proceed through various mechanisms. Noncatalytic, i.e., thermal cracking can occur when hydrocarbons in the absence of a catalyst are brought to high temperatures. Thermal cracking proceeds via primary radicals, which crack at the C–C

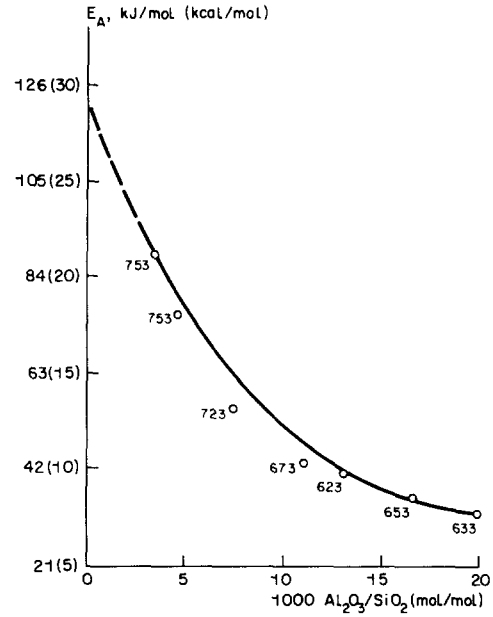

FIG. 5. The effect of alumina content of zeolite MFI on the apparent activation energy of cracking of *n*-hexane. Conditions: P_{tot} = 0.1 MPa; He/*n*-H = 4 mol/mol. Note: Numbers indicate the average temperature (K) of the temperature range in which E_A was determined.

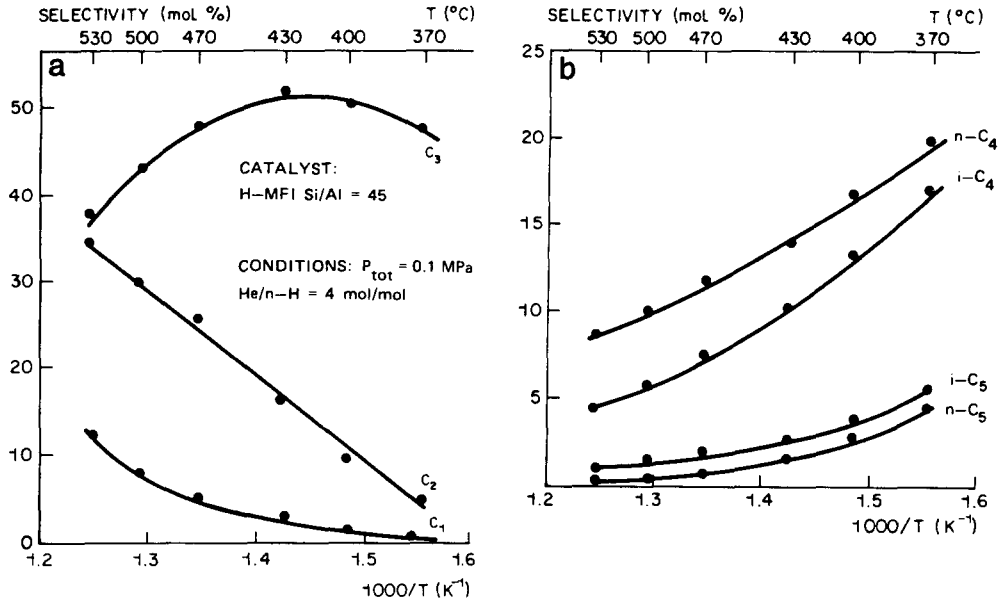

FIG. 6. Selectivity in *n*-hexane cracking as a function of temperature.

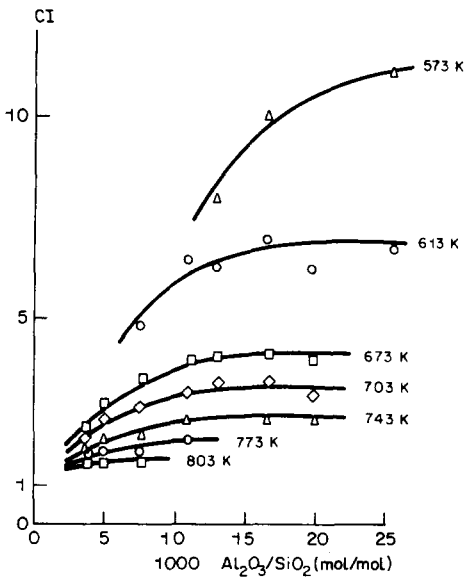

FIG. 7. The constraint index (CI) of zeolite MFI: Effect of alumina content of zeolite and reaction temperature on the ratio of the cracking rates for *n*-hexane and 3-methylpentane. Conditions: P_{tot} = 0.1 MPa; He/(*n*-H + 3-MP) = 4 mol/mol. Two-component feed: He/(*n*-H + 3-MP) = 4 mol/mol; *n*-H/3-MP = 1 mol/mol. Single-component feeds: He/*n*-H = 4 mol/mol; He/3-MP = 4 mol/mol.

bond located β to the carbon atom having the unpaired electron. The repetition of this reaction leads to the formation of large amounts of ethene, and small amounts of methane and α-olefins (*1*). Laboratory experiments of thermal *n*-hexadecane cracking at 773 K established this mechanism (*3*). At higher temperatures (1100–1200 K) small amounts of ethyne are produced (*24*). Although at elevated temperatures thermal cracking is an important pathway for the conversion of hydrocarbon feedstocks, the contribution of the thermal cracking reactions during cracking of the relatively stable hexane isomers at our experimental conditions (temperatures up to 811 K) is negligible. Experiments with both an empty reactor and a reactor loaded with an aluminium-free zeolite (viz. silicalite) did not show any conversion of hexane isomers up to 811 K at a space velocity of 1 g/(g · h).

Catalytic cracking of paraffins can occur either via hydrogenolysis of hydrocarbons over, e.g., Pt or Ni metal particles or via acid catalysis. Since the zeolites used in the present work do not contain metal particles

we can confine the following discussion to purely acid-catalysed conversion of hydrocarbons proceeding via positively charged carbocations, i.e., carbenium ions ($C_nH^+_{2n+1}$) and/or carbonium ions ($C_nH^+_{2n+3}$) as reaction intermediates. The strong dependence of the cracking rates on aluminium content (see, e.g., Fig. 3) supports the conclusion that we are dealing with purely acid-catalysed cracking of *n*-hexane.

If cracking proceeds via the protolytic monomolecular route, the formation of light paraffins (CH_4–C_4H_{10}) can be accounted for by a simple cleavage of a pentacoordinated carbonium ion ($C_6H^+_{15}$) into a smaller alkane (C_nH_{2n+2}) and a classical carbenium ion ($C_mH^+_{2m+1}$) with $n + m = 6$:

$$C_6H_{14} + H\text{–}Z \rightarrow C_6H^+_{15} + Z^- \rightarrow C_3H^+_7 + C_3H_8 + Z^- \quad (1)$$

$$C_6H_{14} + H\text{–}Z \rightarrow C_6H^+_{15} + Z^- \rightarrow C_4H^+_9 + C_2H_6 + Z^- \quad (2a)$$

$$C_6H_{14} + H\text{–}Z \rightarrow C_6H^+_{15} + Z^- \rightarrow C_2H^+_5 + C_4H_{10} + Z^- \quad (2b)$$

$$C_6H_{14} + H\text{–}Z \rightarrow C_6H^+_{15} + Z^- \rightarrow C_5H^+_{11} + CH_4 + Z^-, \quad (3)$$

where H–Z denotes a proton site in the zeolite framework.

Since hydrogen is also observed, reaction (4) probably also proceeds:

$$C_6H_{14} + H\text{–}Z \rightarrow C_6H^+_{15} + Z^- \rightarrow C_6H^+_{13} + H_2 + Z^- \quad (4)$$

In fact, reaction (4) describes the net formation of a carbenium ion from a paraffin by hydride abstraction, in agreement with observations by Kouwenhoven (*25*).

On the basis of the present results it is not possible to identify the structure (either linear or branched) of the carbenium ions and paraffins formed in reactions (1) to (4). In the next step, the carbenium ions formed may lose a proton and form the corresponding olefin:

$$C_nH^+_{2n+1} + Z^- \rightarrow C_nH_{2n} + H\text{–}Z \quad (5)$$

However, it cannot be ruled out that the formation of olefins does not proceed via the consecutive reaction (5) but occurs simultaneously in reactions (1) to (4) according to, e.g.,

$$C_6H_{14} + H\text{–}Z \rightarrow C_6H^+_{15} + Z^- \rightarrow C_4H_8 + C_2H_6 + H\text{–}Z \quad (6)$$

Were cracking to proceed exclusively via reactions (1) to (6), the molar amounts of C_2 and C_4 should be equal. However, our results show that with all zeolites the C_2/C_4 ratio is not unity. Therefore cracking must also occur via a different route. This can be rationalized by assuming that the carbenium ions formed in reactions (1)–(4) become involved in secondary reactions rather than in reaction (5), namely:

Isomerization to branched, tertiary carbenium ions and subsequent H-transfer (7a) followed by β-session (7b)

$$(i, n)\text{-}C_4H^+_9 + n\text{-}C_6H_{14} \rightarrow (i, n)\text{-}C_4H_{10} + n\text{-}C_6H^+_{13} \quad (7a)$$

$$n\text{-}C_6H^+_{13} \rightarrow C_3H^+_7 + C_3H_6 \quad (7b)$$

Alkylation of an olefin with a small carbenium ion (reaction(8a)) followed by β-scission of the formed carbenium ion (8b):

$$C_nH_{2n+1}{}^+ + C_mH_{2m} \rightarrow C_{m+n}H_{2m+2n+1}{}^+ \text{ with } (m + n) \geq 6 \quad (8a)$$

$$C_{m+n}H_{2m+2n+1} \rightarrow \text{cracked products via } \beta \text{ scission.} \quad (8b)$$

Isomerization (9a) followed by H-transfer (9b):

$$n\text{-}C_6H^+_{13} \rightarrow i\text{-}C_6H^+_{13} \quad (9a)$$

$$i\text{-}C_6H^+_{13} + n\text{-}C_6H_{14} \rightarrow i\text{-}C_6H_{14} + n\text{-}C_6H^+_{13} \quad (9b)$$

As a final secondary reaction we mention H-transfer reactions between olefins (formed in reaction (5)), yielding paraffins, diolefins, cycloolefins, and ultimately aromatics. Reactions (7) and (8) illustrate the

classical cracking mechanism where β-scission of a carbenium ion is the characteristic step, which proceeds following either a H-transfer reaction or an alkylation reaction.

The Cracking Mechanism Ratio (CMR)

The above discussion indicates that the product spectrum obtained via the protolytic route (reactions (1)–(6)) is substantially different from that obtained if the classical acid-cracking mechanism prevails (reactions (7)–(9)). The classical cracking route yields primarily butanes (especially isobutane, since the corresponding tertiary carbenium ion is the most stable one) and propene, with little (if any) formation of methane and C_2 hydrocarbons. If the protolytic mechanism is operative, cracking of *n*-hexane results in the formation of hydrogen and linear C_1–C_4 hydrocarbons. With regard to ethene and ethane being typical products of the protolytic cracking route, the following should be noted. Whereas the formation of ethane via protolytic cracking can be readily explained on the basis of reaction 2a, it appears that ethene can only be formed via primary carbenium ions (i.e., reaction (5): $C_2H_5^+ + Z^- \rightarrow C_2H_4 + H\text{–}Z$). Indeed, under conditions where protolytic cracking prevails (high steric constraints in FER (Table 2) and low aluminium contents (Table 3)), relatively high C_2^0/C_2^{2-} ratios are observed. In principle, one can correctly argue that primary carbenium ions can also be formed via the classical cracking route. However, despite the high C_2^0/C_2^{2-} ratio observed under the more demanding conditions, it appears that for zeolites MFI, MOR and US-Y and in a broad compositional range the C_2^0/C_2^{2-} ratio does not strongly vary, i.e., variations in the amounts of ethane and ethene occur concomitantly. This result suggests that the primary carbenium ions necessary to form ethene are more readily generated from pentacoordinated intermediates than via the classical route. Since both the formation of a primary carbenium ion and the formation of a pentacoordinated carbonium ion require a high activation energy, it is conceivable that once a carbonium ion is formed the subsequent formation of a primary carbenium ion is facilitated. Therefore, in addition to C_1 it seems reasonable to regard both ethane and ethene as typical products of the protolytic cracking route, while isobutane is indicative of the classical route.

In order to indicate the relative contributions of the two different cracking mechanisms for *n*-hexane cracking we use a "cracking mechanism ratio" (CMR), which is defind as the ratio $\{(C_1 + \Sigma C_2)/i\text{-}C_4^0\}$, where C_1, ΣC_2, and $i\text{-}C_4^0$ denote the molar selectivities to methane, total C_2 hydrocarbons, and *i*-butane, respectively. We stress that for our present series of *n*-hexane cracking experiments the CMR expresses the relative contributions of two purely acid-catalysed cracking routes. A high value for the CMR (>1) reflects a significant contribution of the protolytic cracking route, while a low value ($0 < CMR < 1$) is indicative of classical carbenium ion chemistry and cracking through β-scission reactions. The CMR is considered to be a useful parameter to reveal in a qualitative manner the extent to which the two acid-catalysed cracking mechanisms prevail. On the other hand, the value of the CMR does not have an absolute significance since the cracking mechanisms are too complicated. For instance, a value of unity for the CMR does not necessarily imply that the two cracking routes are equally important.

Effect of Zeolite Structure on CMR

The results in Fig. 8 show that the CMR decreases with increasing pore dimensions, indicating that with decreasing pore dimensions cracking proceeds more and more via the protolytic route. Furthermore, since especially $i\text{-}C_4$ is a typical product of β-scission reactions (the tertiary carbenium ion is the most stable one), the increase of the $i\text{-}C_4^0/n\text{-}C_4^0$ ratio with the pore dimensions supports this suggestion. The $i\text{-}C_6$ hydrocarbons are formed via isomerization reactions of the intermediate carbenium ions: (again) the se-

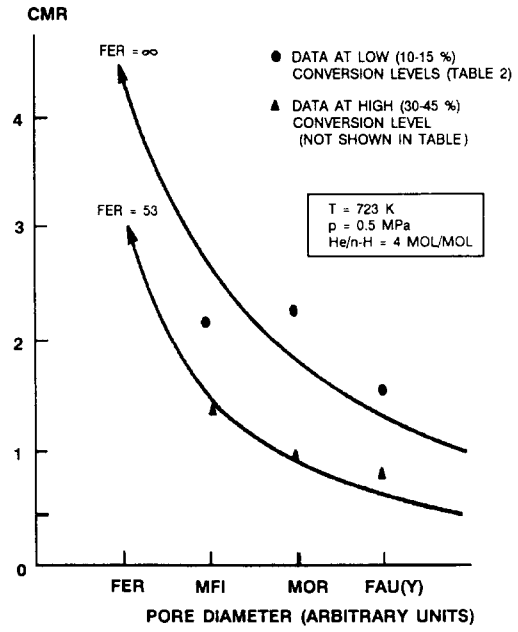

FIG. 8. Variation of cracking selectivity as a function of zeolite structure. *n*-Hexane cracking over different zeolites (Si/Al ≃ 10 mol/mol).

lectivity for the formation of these products increases with the pore dimensions. The increase of the paraffin/olefin (C_4^0/C_4^{2-} and C_3^0/C_3^{2-}) ratio with increasing pore dimension can be accounted for by assuming that H-transfer reactions become more important with increasing pore dimensions. Finally, the importance of the protolytic cracking route with zeolite FER is also reflected in the high selectivity of this zeolite for the formation of hydrogen, methane, and C_2 hydrocarbons. Other investigators have also found that the extent of protolytic cracking is strongly affected by the zeolite structure (*4, 26*).

Since the classical cracking route (proceeding either via a H-transfer reaction followed by β-scission or via alkylation between carbenium ions and olefins followed by β-scission) involves bimolecular reactions, it seems fair to assume that with this reaction the transition-state complex is more bulky than in the case of the monomolecular protolytic cracking reaction. Thus, it would seem justified to relate the relative contributions of the two cracking routes with the pore dimensions of the zeolite involved. Since the dimensions of the transition-state complex of the intermediate in the β-scission route are larger than those of the intermediate involved in the monomolecular cracking reaction, it can be visualized that with zeolite FER cracking proceeds predominantly via the protolytic route, while with MFI, MOR, and FAU (Y) cracking occurs more and more via the classical (β-scission) route. Likewise, it can be explained that the occurrence of secondary (bimolecular) reactions is also strongly dependent on the dimensions of the pores. In the large-pore sieves such as FAU and MOR the relatively high $i\text{-}C_4^0/n\text{-}C_4^0$ ratio reflects the involvement of tertiary C_4 carbenium ions as reaction intermediates in bimolecular hydrogen-transfer reactions. In the medium-pore zeolite MFI with smaller intracrystalline space the formation of bulky bimolecular reaction complexes is suppressed. Hence, the $i\text{-}C_4^0/n\text{-}C_4^0$ ratio in the cracked products is relatively low. Nevertheless, it can be envisaged that in the zeolites with smaller pores classical cracking reactions via less bulky but less stable secondary carbenium ions may still occur. Thus, the formation of C_3 and linear C_4 hydrocarbons during *n*-H cracking over zeolite MFI can be explained on the basis of bimolecular reactions proceeding via secondary carbenium ions. We note that C_3 and linear C_4 can also be formed via protolytic cracking (vide supra). In zeolite FER the dimensions of the intracrystalline channels are slightly smaller than in zeolite MFI and, more importantly, FER has a one-dimensional 10-ring channel structure and does not possess the cavities formed by the intersecting 10-ring channels as in zeolite MFI. As a consequence, bulky bimolecular transition-state complexes cannot be formed in the acid-catalysed cracking of hydrocarbons over zeolite FER and cracking is most likely to proceed via monomolecular transition-state complexes (i.e., carbonium ions) yielding significant amounts of C_1 and C_2 hydrocarbons and hydrogen.

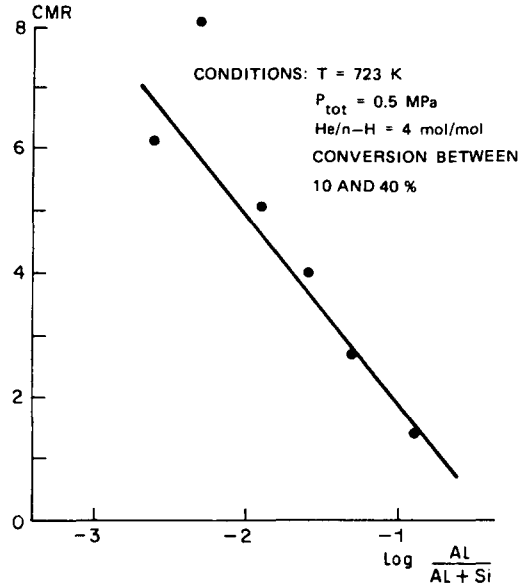

FIG. 9. Variation of selectivity of zeolite H-MFI as a function of aluminium content.

The results shown in Fig. 8 indicate that the CMR is dependent on the conversion level. Since secondary cracking proceeding via classical β-scission becomes more important with increasing conversion levels, it can be readily explained that with increasing conversion level the CMR decreases.

Effect of Aluminium Content of Zeolite MFI on the CMR

Figure 9 shows that the CMR measured for zeolite MFI increases with decreasing aluminium content, indicating that with decreasing aluminium content the contribution of the protolytic cracking route increases as compared to that of the classical β-scission route. Since there is experimental and theoretical evidence in the literature (*16, 27*) which suggests that the intrinsic acidity of the acid sites in zeolite MFI is not dependent on the aluminium concentration, it seems reasonable to conclude that the variation of the CMR with aluminium content cannot be explained on the basis of differences in intrinsic acidity.

Assuming that the hydrogen-transfer process (which appears to be the rate-determining step in the β-scission route (*1*)) requires the presence of two adjacent acid sites (formed by two neighboring lattice aluminium ions) and that the protolytic cracking route can proceed on isolated acid sites, it can be explained that the relative contributions of the two cracking mechanisms depend on the lattice aluminium content. Previously, for zeolite MFI the density of pairs of next-nearest aluminium ions was calculated as a function of the aluminium content and it was shown that the possibility of finding two adjacent sites decreases quadratically with the number of framework aluminium ions (*28*). Accordingly, it can be envisaged that with increasing Si/Al ratio the relative contribution of the monomolecular protolytic cracking route as compared to that of the bimolecular β-scission route increases.

It is, however, difficult to envisage why this bimolecular H-transfer reaction is favoured by the presence of two adjacent acid sites. An explanation for the observed relation between aluminium content and the H-transfer reaction has been proposed by Corma *et al.* (*9, 29*). These authors suggest on the basis of low-temperature adsorption experiments that due to the increasing hydrophobicity of the zeolite lattice with decreasing aluminium content the concentration of olefins (present in the zeolite pores at elevated reaction temperatures) decreases, leading to a suppression of hydrogen-transfer reactions. In fact, this explanation implies that with increasing lattice aluminium content the concentration of carbenium ions in the zeolitic pores increases. It is generally assumed that the carbenium ions present in the zeolite pores are located at the acid centres. In the H-transfer step an incoming paraffin donates a hydride ion to the adsorbed carbenium ion, yielding another paraffin and another carbenium ion. As is (schematically) shown in Fig. 10, it can be envisaged that compared to an isolated acid site the presence of two adjacent acid sites (associated with lattice aluminium ions) stabilizes to a greater extent the transition-state

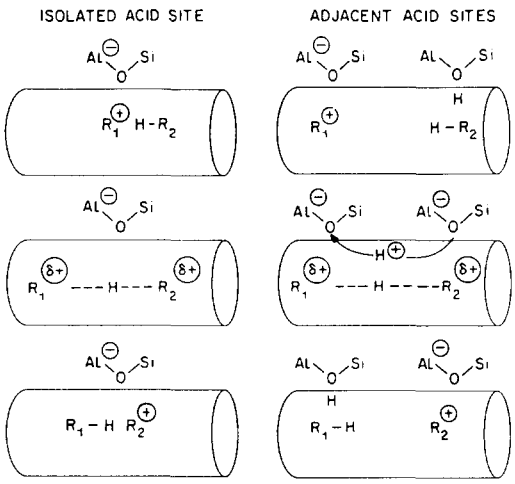

FIG. 10. Tentative scheme to account for the observation that adjacent acid sites in zeolite favour H-transfer reaction.

complex formed during the H-transfer reaction, thus increasing the rate of the H-transfer step, particularly if space constraints in the narrow pores system do not allow an optimal geometrical arrangement of the transition-state complex involved in the hydrogen-transfer reaction. It should be mentioned that during the intermolecular hydrogen-transfer step, a proton associated with one of the acid sites will move to the adjacent site. Further work is necessary to support this model.

Effect of Aluminium Content and Temperature on n-Hexane Cracking Rate over Zeolite MFI

We have argued above that with decreasing aluminium content cracking proceeds more and more via the protolytic route. This conclusion also offers an explanation for the variation in activation energy with the aluminium content of zeolite MFI (Fig. 5). Since the activation energies for the various MFI samples differing in the aluminium content have been measured in different temperature intervals, it appears that in Fig. 5 the variation of the activation energy is caused not only by the change in the lattice aluminium concentration but also by the differences in reaction temperatures. As discussed above, both effects appear to influence the relative contribution of the two cracking mechanisms leading to a continuous decrease in activation energy with increasing aluminium content and decreasing reaction temperature. Accordingly, the data in Fig. 5 suggest that the activation energy for protolytic cracking (occurring at low Al content and/or elevated temperatures) is higher than that of the classical route: a value of at least 90 kJ/mol can be inferred from Fig. 5 for cracking at high temperature over silica-rich MFI, while at lower temperatures cracking over aluminium-rich MFI samples occurs with an activation energy as low as about 30 kJ/mol. Thus, compared to the classical cracking route the protolytic route proceeds with a higher activation energy and via a transition-state complex with smaller dimensions (lower volume of activation).

Although to the best of our knowledge basic experimental data on the activation energies of the rate-determining steps in the two *n*-hexane cracking routes are not available, the data reported by Brouwer and Hogeveen (*8*) may give an indication of the activation energies of these two cracking routes. Studying the chemistry of carbocations in liquid acids (such as $HF–SbF_5$) these authors found for the hydrogen transfer from a secondary carbon atom to a tertiary carbenium ion an activation energy of about 55 kJ/mol and for the hydrogen transfer from a tertiary carbon atom to a tertiary carbenium ion a value of about 12 kJ/mol. Since it is generally assumed that hydrogen transfer is the rate-limiting step in the classical β-scission route (*1*), it can be argued that the activation energy for β-scission is equal to or lower than 55 kJ/mol, in agreement with our observations. By contrast, it was found that protolytic cracking of neopentane to *tert*-butyl cations and methane requires an activation energy of about 88 kJ/mol.

Figure 11 shows that the CMR for *n*-H cracking over zeolite MFI increases with increasing temperature, indicating an in-

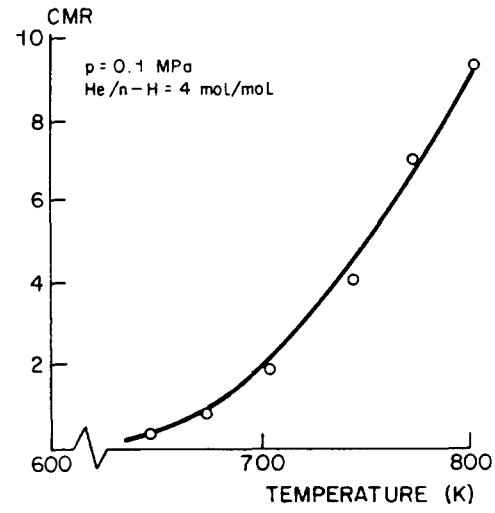

FIG. 11. Variation of selectivity of H-MFI (Si/Al = 21) with reaction temperature.

creasing contribution of the protolytic cracking route with increasing temperature. This finding can be explained on the basis of the higher activation energy for protolytic cracking as compared to the classical β-scission route.

Our results show that with decreasing temperature the rate constant more than proportionally increases with the aluminium content (Fig. 4). In fact, the order in the aluminium content varies from 1 (at 811 K) to about 2 (at 623 K), supporting the conclusion that the bimolecular classical route requires (as suggested above) the presence of two neighbouring acid sites. Thus, at low temperatures cracking mainly proceeds via the classical route and as a consequence the cracking activity increases with the number of adjacent acid sites. Although usually with silicon-rich (Si/Al $>$ 10) zeolites it is assumed that the cracking rate varies linearly with aluminium content, our present results show that this assumption is only justified at relatively high temperatures (at or above 811 K), where the protolytic cracking mechanism, which requires only isolated acidic sites, dominates.

Finally, we note that although the order in the aluminium content varies with temperature, the results shown in Fig. 1 and the available literature data (*16*) indicate that in the entire temperature range 573–811 K (300–538°C) the cracking rate is first-order in *n*-hexane. If the H-transfer reaction between a carbenium ion and a *n*-hexane molecule is indeed the rate-limiting step for the classical cracking route a second-order dependence of the cracking rate on the *n*-hexane concentration would be expected. However, our results show that independent of the mode of cracking the rate can be described by a first-order model. With regard to the classical route this would suggest that for a particular zeolite the concentration of the carbenium ions (located at the lattice aluminium ions) is virtually independent of the *n*-hexane pressure. Accordingly, it can be explained that although the cracking rate of the classical route shows a first-order dependence on the *n*-hexane concentration, the cracking rate exhibits a second-order dependence on the lattice aluminium concentration since the presence of two adjacent Al-ions would favour (on the basis of the model in Fig. 10) the H-transfer reaction.

The Constraint Index of Zeolite MFI

On the basis of the concept that the relative contributions of the two cracking routes vary with the aluminium content, an explanation can be given for the variation of the constraint index of zeolite MFI with aluminium content and temperature (Fig. 7). In zeolite MFI the difference between the cracking rates of *n*-H and 3-MP are related to differences in the dimensions of the transition-state complexes formed during cracking of these two compounds. It has been suggested that the transition-state complex formed upon 3-MP cracking is bulkier than the one formed upon *n*-H cracking (*30*). Since the reaction takes place in the narrow pores of zeolite MFI, the formation of the bulkier 3-MP transition-state complexes sterically more hindered than the formation of the *n*-H transition-state complex. As a result, with zeolite MFI (at standard test conditions (*13, 14*)) the cracking rate is higher

for *n*-H than for 3-MP, leading to a CI above unity. Figure 7 shows that, irrespective of the reaction temperature, with decreasing aluminium content the CI decreases and ultimately approaches 1. Our argument that, with decreasing aluminium content, cracking proceeds to an increasing extent via the monomolecular protolytic route gives an explanation for this observation. Since the protolytic cracking route is a monomolecular reaction, it can be argued that the transition-state complex formed in the protolytic cracking route is less bulky than the one formed in the classical cracking route. Thus, when cracking proceeds more and more via the protolytic route (which is the case with decreasing lattice aluminium content), it can be easily envisaged that during cracking of *n*-H and 3-MP the effect of sterical constraints imposed by the zeolite lattice decreases, leading to a lower CI.

As has also been suggested by Haag and Dessau (*4*), the concept that the relative contributions of the two cracking routes vary with temperature can (at least partly) explain the variation of the CI of MFI with temperature (*14*). With decreasing temperature cracking proceeds more and more via the bimolecular classical route (proceeding via bulkier intermediates than in the case of the monomolecular route), yielding a higher CI.

CONCLUSIONS

The present results show that the mode of *n*-hexane cracking over zeolites varies with the aluminium content and the structure of the zeolite and with the reaction temperature. The relative contributions of the two acid-catalysed cracking routes encountered is expressed by the cracking mechanism ratio. A high value of this index indicates a relatively high contribution of the protolytic cracking route involving carbonium ions, whereas a low value is indicative of the classical β-scission route involving classical carbenium ions as intermediates. With increasing temperature, decreasing aluminium content and decreasing pore dimensions as studied with the zeolites FAU, MOR, MFI, and FER, the relative contribution of the (monomolecular) protolytic cracking route increases compared to the (bimolecular) classical route. On the basis of these results the variation of the Constraint Index of zeolite MFI with aluminium content and reaction temperature can be easily rationalized. Furthermore, the present results also give an explanation for the variation of the activation energy of cracking of *n*-hexane with aluminium content over zeolite MFI. Finally, it is tentatively concluded that the classical cracking route is favoured by the presence of two neighbouring acid sites and lower reaction temperatures. As a result, the relation between the reaction rate constant and the lattice aluminium content changes with the reaction temperature. Whereas at 811 K the cracking constant varies linearly with the aluminium content, the order in the aluminium content increases to about 2 at 623 K.

ACKNOWLEDGMENTS

The authors express their appreciation to Mr. J. H. E. Glezer for technical assistance in the experimental work. Furthermore, the authors are indebted to Dr. A. L. Farragher and Dr. Ir. S. T. Sie for stimulating discussions and their critical comments on the manuscript.

REFERENCES

1. Gates, B. C., Katzer, J. R., and Schuit, G. C. A., "Chemistry of Catalytic Processes," p. 1. McGraw–Hill, New York, 1979.
2. Thomas, C. L., *Ind. Eng. Chem.* **41,** 2564 (1949).
3. Greensfelder, B. S., Voge, H. H., and Good, G. M., *Ind. Eng. Chem.* **41,** 2573 (1949).
4. Haag, W. O., and Dessau, R. M., *Proc. Int. 8th Congr. Catal., Berlin, 1984* **2,** 305 (1984).
5. Corma, A., Planelles, J., Sanchez-Marin. J., and Thomas, F., *J. Catal.* **93,** 30 (1985).
6. Abbot, J., and Wojchiechowski, B. W., *Canad. J. Eng.* **66,** 825 (1988).
7. Olah, G. A., Halpern, Y., Shen, J., and Mo, Y. K., *J. Amer. Chem. Soc.* (a) **95,** 4960 (1973); (b) **93,** 1251 (1971).
8. Brouwer, D. M., and Hogeveen, H., *Prog. Phys. Org. Chem.* **9,** 179 (1972).
9. Corma, A., and Orchilles, A. V., *J. Catal.* **115,** 551 (1989).
10. Corma, A., *Stud. Surf. Sci. Catal.* **49,** 49 (1989).
11. Gianetto, G., Sausare, S., and Guisnet, M., *J. Chem. Soc. Chem. Commun.*, 302 (1986).

12. Mirodatos, C., and Barthomeuf, D., *J. Catal.* **114,** 121 (1989).
13. See, e.g., US patent 4,034,053 to Mobil Oil (1977).
14. Frillette, V. J., Haag, W. O., and Lago, R. M., *J. Catal.* **67,** 218 (1981).
15. US patent 3,702,886 to Mobil Oil (1972).
16. (a) Haag, W. O., Lago, R. M., and Weisz, P. B., *Nature (London)* **309,** 589 (1984); (b) Olson, D. H., Haag, W. O., and Lago, R. M., *J. Catal.* **61,** 390 (1980).
17. Kikuchi, E., Nakano, H., Shimomura, K., and Morita, Y., *Sekiyu Gakkaishi* **28,** 210 (1985).
18. Rastelli, H., Lok, B. M., Duisman, J. A., Earls, D. E., and Mullhaupt, J. T., *Canad. J. Chem. Eng.* **60,** 44 (1982).
19. Lombardo, E. A., Gaffney, T. R., and Hall, W. K., *in* "Proceedings 9th Int. Conf. Catal., Calgary 1988)" (M. J. Phillips and M. Ternan, Eds.), Vol. 1, p. 412. Chemical Institute of Canada, Ottawa, 1988.
20. Derouane, E. G., André, J. M., and Lucas, A. A., *J. Catal.* **110,** 58 (1988).
21. Derouane, E. G., *J. Catal.* **100,** 541 (1986).
22. Wielers, A. F. H., and Post, M. F. M., in press.
23. Post, M. F. M., Van Amstel, J., and Kouwenhoven, H. W., *in* "Proc. 6th Int. Zeolite Conf. (Reno 1983)," p. 517. Butterworths, Guildford, 1984.
24. Prescott, J. H., *Chem. Eng.* **7,** 52 (1975).
25. Kouwenhoven, H. W., *Adv. Chem. Ser.* **121,** 529 (1973).
26. Planelles, J., Sanchez-Marin, J., Thomas, F. and Corma, A., *J. Mol. Catal.* **32,** 365 (1985).
27. Barthomeuf, D., *Mater. Chem. Phys.* **17,** 49 (1987).
28. Den Ouden, C. J. J., Wielers, A. F. H., Kuipers, H. P. C. E., Vaarkamp, M., Mackay, M., and Post, M. F. M., *Stud. Surf. Sci. Catal.* **49,** 825 (1989).
29. Corma, A., Faraldos, M. and Mifsud, A., *Appl. Catal.* **47,** 125 (1989).
30. Haag, W. O., Lago, R. M., and Weisz, P. B., *Faraday Discuss. Chem. Soc.* **72,** 317 (1981).